AD-A062 866 MINNESOTA UNIV MINNEAPOLIS HEAT TRANSFER LAB F/G 21/5
HEAT TRANSFER PROBLEMS IN ADVANCED GAS TURBINES FOR NAVAL APPLI--ETC(U)
NOV 78 E R ECKERT, R J GOLDSTEIN, E M SPARROW N00014-76-C-0246

UNCLASSIFIED NL

1 OF 1
ADA
062866

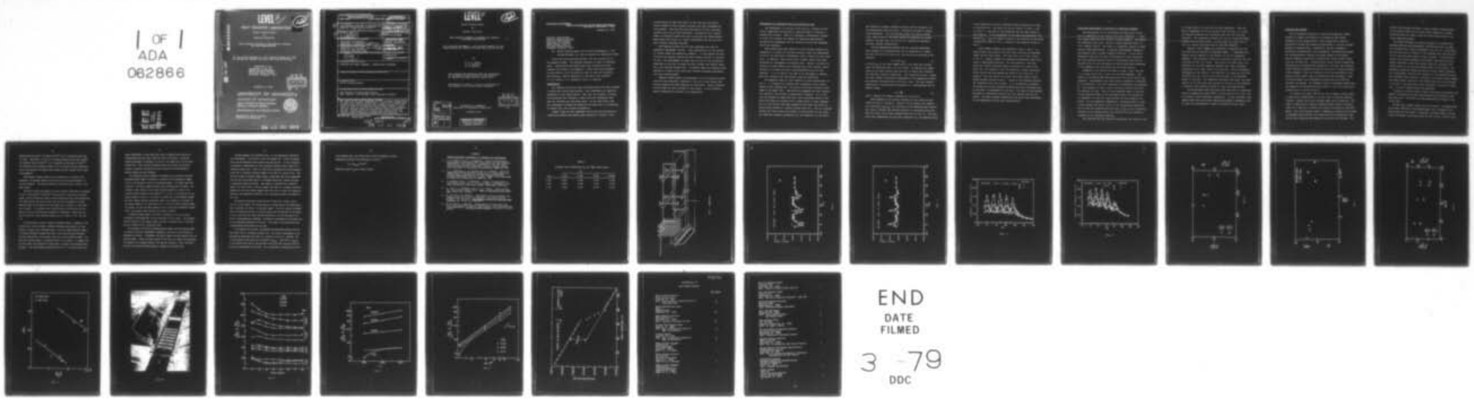

END
DATE
FILMED
3-79
DDC

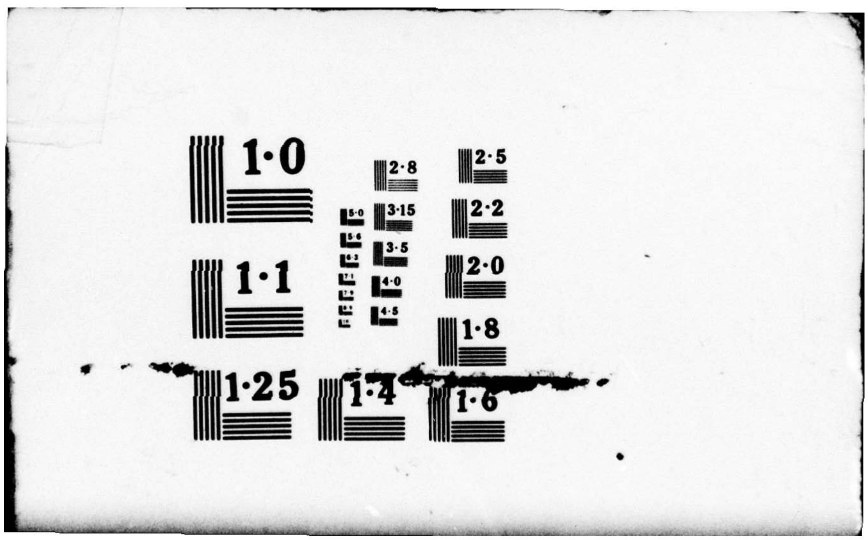
1·0
2·8
2·5
3·15
2·2
5·0
5·6
6·3
3·5
2·0
1·1
4·0
4·5
1·8
1·25
1·4
1·6

HEAT TRANSFER LABORATORY

Annual Progress Report
on
Research concerning

"Heat Transfer Problems in Advanced Gas Turbines for Naval Applications"

for the period September 1, 1977 through November 30, 1978 on contract No. N00014-76-C-0246, Work Unit NR 097-383.

Submitted to the
DEPARTMENT OF THE NAVY
Office of Naval Research
800 North Quincy Street
Arlington, Virginia 22217

November 30, 1978

UNIVERSITY OF MINNESOTA
INSTITUTE OF TECHNOLOGY
School of Mechanical and Aerospace Engineering
Department of Mechanical Engineering
MINNEAPOLIS, MINNESOTA 55455

SECURITY CLASSIFICATION OF THIS PAGE (When Data Entered)

REPORT DOCUMENTATION PAGE

READ INSTRUCTIONS BEFORE COMPLETING FORM

1. REPORT NUMBER

2. GOVT ACCESSION NO.

3. RECIPIENT'S CATALOG NUMBER

9

4. TITLE (and Subtitle)

6

HEAT TRANSFER PROBLEMS IN ADVANCED GAS TURBINES FOR NAVAL APPLICATIONS.

5. TYPE OF REPORT & PERIOD COVERED

Annual Progress Report, ~~9/1/77 - 11/30/78~~

6. PERFORMING ORG. REPORT NUMBER

1 Sep 77-30 Nov 78

7. AUTHOR(s)

10

E. R. G. Eckert,
R. J. Goldstein
E. M. Sparrow

8. CONTRACT OR GRANT NUMBER(s)

15

N00014-76-C-0246

9. PERFORMING ORGANIZATION NAME AND ADDRESS

University of Minnesota
Department of Mechanical Engineering
Minneapolis, Minnesota 55455

10. PROGRAM ELEMENT, PROJECT, TASK AREA & WORK UNIT NUMBERS

Approved for public release, distribution unlimited.

11. CONTROLLING OFFICE NAME AND ADDRESS

Department of the Navy, Code 473
Office of Naval Research
Arlington, Virginia 22217

11 30

12. REPORT DATE

November 20, 1978

13. NUMBER OF PAGES

30

14. MONITORING AGENCY NAME & ADDRESS (if different from Controlling Office)

12 44p.

15. SECURITY CLASS. (of this report)

UNCLASSIFIED

15a. DECLASSIFICATION/DOWNGRADING SCHEDULE

16. DISTRIBUTION STATEMENT (of this Report)

APPROVED FOR PUBLIC RELEASE: DISTRIBUTION UNLIMITED.

17. DISTRIBUTION STATEMENT (of the abstract entered in Block 20, if different from Report)

18. SUPPLEMENTARY NOTES

Annual Progress Report

19. KEY WORDS (Continue on reverse side if necessary and identify by block number)

Gas Turbines for Naval Applications
Heat transfer, film cooling, heat exchanger surfaces.

20. ABSTRACT (Continue on reverse side if necessary and identify by block number)

The report covers heat exchanger studies stressing measurements of local heat transfer coefficients. Direct heat transfer measurements have been performed and a method has also been used which is based on the heat and mass transfer analogy. Local ablation rates are obtained on a model covered with napthalene and heat transfer rates are deduced from these through the analogy. Measurements of the turbulence intensity in a gas stream leaving a combustion chamber are also reported.

DD FORM 1 JAN 73 1473 EDITION OF 1 NOV 65 IS OBSOLETE
S/N 0102-LF-014-6601

UNCLASSIFIED
SECURITY CLASSIFICATION OF THIS PAGE (When Data Entered)

165 400

78 12 29 009

LEVEL II

(12)

Annual Progress Report

of

Research concerning

HEAT TRANSFER PROBLEMS IN ADVANCED GAS TURBINES FOR NAVAL APPLICATIONS

for the period September 1, 1977 through November 30, 1977
under contract No. N00014-76-C-0246, Work Unit NR 097-383

by

E. R. G. Eckert
R. J. Goldstein
E. M. Sparrow

This research was conducted under the sponsorship of the Office of Naval Research under Contract No. N00014-76-C-0246, Work Unit NR 097-383.

UNIVERSITY OF MINNESOTA
Department of Mechanical Engineering

November 1978

University of Minnesota
School of Mechanical and Aerospace Engineering
Minneapolis, Minnesota 55455

November 30, 1978

Director, Power Branch
Material Sciences Division
Office of Naval Research
~~Department of the Navy~~
Power Program, Code 473
800 North Quincy Street
Arlington, Virginia 22217

Re: Annual progress report for the period September 1, 1977 through November 30, 1978 on contract No. N00014-76-C-0246.

During the above mentioned period, work was carried out in two research phases. The progress obtained in those is discussed below. Publications and theses which have resulted from this research are listed in the Appendix. Copies have been forwarded to your office or will be mailed as soon as they are available. The following faculty members are involved in this research: E. R. G. Eckert, R. J. Goldstein, and E. M. Sparrow.

INTRODUCTION

Our research during the above mentioned period has been directed to marine gas turbine applications. Heat exchangers are important components in such power plants. They can, for instance, increase the efficiency and, therefore, reduce the fuel consumption when they are inserted into the power cycle. On the other hand, such heat exchangers increase the weight of the plant and it is important to reduce their size as much as possible.

Compact types of heat exchangers which have been developed by industries minimize the surface area required to transfer a pre-

scribed amount of heat and reduce in this way size and weight. Various shapes of heat transfer surfaces have been developed for this process. This has been done empirically and the individual surfaces have not yet been optimized. One phase of our research effort is directed toward this goal by accurate and local measurements which will result in a basic understanding of the flow and heat transfer processes involved.

The required surface area of heat exchangers can also be reduced by impingement cooling. Other applications are the cooling of turbine blades and combustion chambers. In this method the cooling fluid is directed towards the heat transfer surface in the form of jets. The impingement of these jets, as well as the turbulence generated in this way, increase the heat transfer and reduce, therefore, the required surface area. A research phase has therefore been devoted to a study of the local heat transfer processes associated with this cooling method.

Research aimed towards the measurement of the turbulent fluctuations and the turbulence intensity at the exit of gas turbine combustion chambers has been underway for some years. Results obtained in this study are also included in this report. A more extensive report discussing the results is in preparation.

Impingement of a Multiple Array of Circular Air Jets

The impingement of an array of air jets on a surface of different temperature can provide an effective means of cooling or heating that surface. There is, therefore, considerable interest in using this process in a number of industrial applications, including heat exchangers and the cooling of electrical equipment and of gas turbines.

Many studies have been devoted to heat transfer caused by impingement of a single jet and more recently, under the sponsorship of ONR at the University of Minnesota, from a single jet with cross flow. In addition, some overall heat transfer results have been published for impingement of multiple jets. However, virtually no studies are known dealing with detailed local heat transfer distributions on a surface on which a two-dimensional array of jets impinges. It is to fulfill this gap in our knowledge on impingement heat transfer that the present study was undertaken.

The apparatus used for this research is shown schematically in Fig. 1. It consists of a channel with rectangular cross section closed on the lefthand end. An array of five rows of holes is provided in the upper wall. The holes are staggered and their centers are located at the corners of equilateral triangles. Air is fed into the channel by tubes with their axis orientated normal to the walls and ending in orifices with a length equal to their diameter. The air jets leaving the holes impinge on the lower wall which is electrically heated to a locally uniform heat flux. The air injected through the holes leaves the channel in the direction to the right. The important geometric parameters are the diameter D of the holes,

the distance S between neighboring holes, and the distance L of the heated plate from the holes. Provisions are made to change these parameters. The jet Reynolds number can also be varied. Local temperatures on the lower heated wall measured by thermocouples, the heat flux, and the jet air temperature determine the heat transfer coefficients.

Initial measurements showed that the relation describing heat transfer on the heated plate can be presented in a simple way when the heat flux q per unit time and area is defined by the equation:

$$q = h(T_w - T_{ad}) \tag{1}$$

in which T_{ad} is the local temperature of the upper wall surface under the condition that it is not heated. T_w denotes the temperature at the same location when the wall is heated and h denotes the film heat transfer coefficient. The formulation of Eq. 1 makes the heat transfer coefficient independent of the temperature difference between the heated wall and the air jets. The heat transfer coefficient is conventionally presented in a dimensionless form as Nusselt number

$$Nu = \frac{hD}{k} \tag{2}$$

where k denotes the thermal conductivity of the air.

Some examples of the results obtained in this study are presented in Figs. 2 through 5. Figures 2 and 3 present the temperature difference $T_{ad} - T_{jet}$ as a function of the dimensionless location x/D, where x denotes the distance measured in downstream direction from the first row of holes (counted from left in Fig. 1). The adiabatic wall temperature and the wall temperature T_w are measured along

a line starting at a point vertically below the center of a hole in the first row. The ratio L/D has the value 2 in Fig. 2, and 5 in Fig. 3. The rest of the parameters has the same values in both figures. It is interesting to note that the temperature difference $T_{ad} - T_{jet}$ has negative values at the location of the holes indicated by arrows in Fig. 2, whereas it has positive values in Fig. 3.

Local Nusselt numbers are presented in Figs. 4 and 5. In these figures the ratio L/D has the value 5 and the jet Reynolds number has the value 15000. The ratio S/D is 8 in Fig. 4 and 4 in Fig. 5. Nusselt numbers are presented as measured along three lines in downstream direction. For the location 0, the line starts at a point vertically above the center of a tube of the first row. For location 2 the line starts at a point vertically below a point half-way between two holes of the first row. At location 1 the line starts at a point vertically below a point midway between location 0 and 2. Arrows on the abscissa indicate the location of the row of holes. It is interesting to observe the maxima of the heat transfer coefficients which obviously occur at the point of impingement of the jets. The value of the maximum decreases in downstream direction (in the figures from left to right). The heat transfer coefficients are quite high testifying to the advantage of using this cooling method.

Turbulence Measurements at the Exit of Combustion Chambers

The measurements of the turbulence characteristics at the exit of combustors of gas turbines have been completed. A report and a paper describing the results is being prepared. Two different combustors were used. One has a simple premixed flame in a 2 in. diameter burner. The other is a combustor typical to those used for VTOL applications. A special laser-Doppler anemometer was designed which includes frequency shifting. It was used to determine velocities and their fluctuations in axial direction. The time averaged velocity $\bar{u}$ and its fluctuations described by the mean value u', were determined at various positions downstream of the combustor exit and across the exit cross section.

Examples of the results are shown in Figs. 6 and 7 for the 2 in. burner and in Fig. 8 and 9 for the VTOL combustor. The values in the figures have been measured on the center line of the combustor. Measurements were taken without combustion (indicated by the subscript c) and with combustion (indicated by the subscript h). The abscissa in Figs. 6 and 8 is the air-to-fuel ratio A/F, the abscissa in Figs. 7 and 9 is the Reynolds number at the exit of the combustor based on the time mean center line velocity $\bar{u}$, the diameter D of the exit cross section and the kinematic viscosity ν at the respective temperature. The data points in Figs. 6 and 8 present the ratio u'_h/u'_c of the fluctuating velocities for hot and cold condition and the ratio $u'_h/\bar{u}_h$ of the fluctuating velocity to the average center line velocity for hot condition, referred to as turbulence intensity.

One observes that the velocity fluctuations are larger in the

hot stream than in the cold one for both combustors. They are fairly independent of the air-to-fuel ratio for the 2 in. burner but decrease strongly with increasing fuel ratio for the VTOL combustor. The turbulence intensity for the hot stream decreases slightly with air-fuel ratio. It has a value of around 14% for the 2 in. burner and around 17% for the VTOL combustor.

Figures 7 and 9 compare the turbulence intensities for hot and cold flow on the basis of Reynolds number. A remarkable difference can be observed in the behavior of the two combustion chambers. The turbulence levels are practically equal for hot and cold flow in the 2 in. burner. They are, on the other hand, very different for the VTOL combustor because very large turbulence intensities, up to 40%, occur in the cold flow. This is probably a consequence of two factors. The mass flow is larger for cold flow condition than for the hot flow condition even if the Reynolds number is the same. The combustion processes also cause an acceleration of the flow from the entrance to the exit of the combustor, a condition which generally leads to lower turbulence levels.

The measurements described above have been taken in combustion gases at temperatures above 400°C, at flow rates up to 70 m/s, and at unusually large turbulence intensities. It has, therefore, been demonstrated that, with proper design, laser-Doppler anemomentry can be used for measurements in highly fluctuating hot gas flows.

Interrupted Wall Passages

The use of periodic interruptions in plane, flow-aligned heat transfer surfaces is a commonly used technique for increasing the heat transfer coefficients in heat exchange devices. These surfaces may be viewed as a succession of colinear plate segments oriented parallel to the flow, with gaps between the successive plates. Alternatively, they may be regarded as periodically interrupted walls, and the designation, interrupted-wall passages, will be employed here to describe flow passages bounded by such surfaces. Practical examples of periodically interrupted heat transfer surfaces include strip fins and offset fins. Information about the heat transfer--pressure drop characteristics of interrupted-wall passages has, in the main, been confined to overall coefficients obtained from tests on either actual or large-scale models of heat exchangers. While this information is of direct applicability in the design of certain specific types of interrupted-wall heat exchangers, it does not provide insights into the fundamental processes that occur within the individual flow passages. The fundamental studies of interrupted surfaces which have appeared in the literature have been limited to a pair of co-linear plates aligned parallel to the flow direction.

If, instead of two plates, there was an array of numerous, equally spaced co-linear plates aligned parallel to the flow, then, at sufficient downstream distances, a special type of fully developed regime would be established. This regime is characterized by identical developing boundary layers on successive plates and, in addition, by identical flow fields in the successive inter-plate spaces. Such a fully developed regime is fundamentally different from the regime of unchanging velocity profiles that characterizes fully developed duct flows. The new type of regime has been referred to as periodic fully developed. The

periodic fully developed flow admits a periodic thermally developed regime. If the successive plates are at the same uniform temperature, a suitably defined per-plate heat transfer coefficient should become constant at sufficient downstream distances.

The thermal development and ultimate attainment of the periodic fully developed regime has been experimentally investigated here for a co-linear array of plates that is shown in photographic view in Fig. 10. As seen there, the multi-plate array is situated in a flat rectangular duct (the top wall of the test section has been removed to reveal the plates). To facilitate the research, mass transfer experiments were performed rather than direct heat transfer experiments, and the mass transfer results were converted to heat transfer results via the well-known analogy between the two processes. The naphthalene sublimation technique was used for the mass transfer experiments and, correspondingly, each test plate consisted of a thin naphthalene coating which enveloped a metal substrate. According to the heat/mass transfer analogy, the thermal boundary condition for heat transfer plates that would correspond to the plates of the present mass transfer experiments is uniform wall temperature. Air was the working fluid for the experiments.

In addition to the mass transfer studies, axial pressure distributions were measured to determine the pressure drop associated with the presence of the multi-plate array. These results are made dimensionless with respect to the velocity head.

The heat (mass) transfer results will now be presented. The dimensionless mass transfer coefficient is the Sherwood number, which corresponds to the Nusselt number for heat transfer. Furthermore, the Schmidt number Sc for mass transfer corresponds to the Prandtl number for heat transfer. With the aim of

generalizing the results, the quantity $Sh/Sc^{0.4}$ will be presented rather than Sh itself. Furthermore, in view of the analogy between heat and mass transfer, the numerical values of $Sh/Sc^{0.4}$ will be regarded as being equal to $Nu/Pr^{0.4}$. The ordinates of the forthcoming figures will be labelled with both quantities, and in the discussion the phrases heat transfer and mass transfer will be used interchangeably.

The heat/mass transfer results will be presented as a function of two parameters, the Reynolds number Re and the ratio of the plate thickness t to the plate length L. The spacing between the successive plates is equal to the plate length.

The plate-by-plate development of the heat transfer coefficient is presented in Fig. 11, where $Nu/Pr^{0.4}$ and $Sh/Sc^{0.4}$ are plotted as a function of the plate number (1 and 8 respectively denote the most upstream and most downstream plates). The figure contains four sets of data, each of which corresponds to a given Reynolds number in the range from 13,600 (upper part of graph) to 1,000 (lower part of graph). To facilitate their identificaiton, the data points for the successive sets are alternatively blackened or unblackened. Within each set, data are given for three thickness-length ratios t/L equal to 0.04, 0.08, and 0.12.

The figure shows an orderly thermal development whereby, subsequent to the second plate, the heat transfer coefficient decreases monotonically and then attains a constant, fully developed value. At the two higher Reynolds numbers, the thermal development becomes less rapid as the plate thickness decreases, and this trend persists in an overall sense for the third Reynolds number. For the lowest Reynolds number, a different pattern is in evidence. It appears that the flow passes from turbulent to transitional to laminar with decreasing plate thickness. The transitional distribution curve for $t/L = 0.08$ was found to be

highly reproducible, so that data from a pair of repeated runs could not be distinguished from each other within the scale of the figure. In general, thermal development is attained at or prior to the eighth plate for the cases studied here. Since the fully developed values are the ones that are most relevant to practice, attention will now be focused on how they depend on Reynolds number and plate thickness.

The influence of plate thickness is presented in Fig. 12, where the fully developed Nusselt number is plotted as a function of the thickness-to-length ratio t/L for parametric values of the Reynolds number. The figure shows that, in general, the Nusselt number increases with increasing plate thickness. The increase is most dramatic at the lowest Reynolds number as a result of the thickness-induced change in flow regime (i.e., the t/L = 0.04 plates are in the laminar regime, and the t/L = 0.08 and 0.12 plates are in the turbulent regime). With this laminar-turbulent transition, there is an increase of 65 percent in the Nusselt number as t/L varies from 0.04 to 0.12 at the lowest Reynolds number. If, however, the flow had been turbulent for all three plate thicknesses (dashed line), the thickness effect would be only about 12 percent.

At higher Reynolds numbers, the flow is turbulent for all of the plate thicknesses investigated here, so that transition is not a factor. The thickness-related increases in the Nusselt number are about 20 percent for Re = 3,900 and about 40 percent for Re = 8,200 and 13,600.

The variation of the fully developed Nusselt number with the Reynolds number is plotted in Fig. 13 on logarithmic coordinates, with the t/L ratio serving to parameterize the data. As expected, the Nusselt number increases markedly with the Reynolds number. Within the small scatter of the data, a straight line representation appears to be adequate except at the smallest thickness. There, the rapid drop-off at the lowest Reynolds number is suggestive of laminar flow.

The main message to be conveyed by Fig. 13 is the augmentation afforded by the interruptions. To this end, a short line segment (Re > 10,000) corresponding to the Dittus-Boelter (D-B) equation has been plotted. If the D-B equation is accepted as representing the fully developed turbulent Nusselt number for a continuous-walled duct , then it is seen that the presence of the interruptions gives rise to increases in Nusselt number on the order of a factor of two. This two-fold increase in Nusselt number enables a given heat load to be accommodated with only half the surface area of a continuous-walled duct, thereby resulting in substantial materials savings. With regard to turbulent flow at Reynolds numbers less than 10,000, it does not appear that there is a reliable correlation equation for duct-flow Nusselt numbers which can serve as a basis for comparison. Therefore, the augmentation afforded by the interruptions cannot be estimated at this time.

The pressure distribution along the duct is shown for a typical case in Fig. 14. In this figure, the static pressure is plotted against the dimensionless axial coordinate x/L, where L is the plate length. The axial stations corresponding to the beginning and end of the multi-plate array are indicated in the figure. As can be seen from the linear pressure distribution, the flow upstream of the array is hydrodynamically developed. Furthermore, hydrodynamically developed flow is re-established downstream of the array. The slopes of the upstream and downstream pressure distributions are the same.

In the absence of the array, the upstream and downstream pressure distributions would lie on a continuous straight line. The vertical displacement of the upstream and downstream lines that is in evidence in Fig. 11 is, therefore, due to the presence of the array and is denoted by Δp_{array}. Specifically, Δp_{array} is the pressure drop that is over and above that which would otherwise exist in the duct in the absence of the array. For a dimensionless representation of the

array pressure drop, the velocity head $(1/2)\rho V^2$ is employed, so that a dimensionless pressure loss coefficient is given by

$$K_p = \Delta p_{array}/(1/2)\rho V^2$$

Numerical values of K_p are listed in Table 1.

APPENDIX

Papers published, presented, or accepted for publication

1.) M. Y. Jabbari and R. J. Goldstein: "Effect of Mainstream Acceleration on Adiabatic Wall Temperature and Heat Transfer Downstream of Gas Injection," presented at the 6th International Heat Transfer Conference, Toronto, Canada, August, 1978, published in Conference Proceedings as Paper No. 134.

2.) R. J. Goldstein, V. L. Eriksen and J. W. Ramsey: "Flow and Temperature Fields Following Injection of a Jet Normal to a Cross Stream," presented at the 6th International Heat Transfer Conference, Toronto, Canada, August, 1978, published in Conference Proceedings as Paper No. 133.

3.) K. Kadotani and R. J. Goldstein: "Effect of Mainstream on Jets Issuing from a Row of Inclined Holes," presented at the 1978 Gas Turbine Conference, London, ASME paper 78-GT-138.

4.) S. Ito, R. J. Goldstein and E. R. G. Eckert: "Film Cooling of a Gas Turbine Blade, Trans. ASME, J. Engineering for Power, 100, (1978), pp. 476-481.

5.) N. Cur and E. M. Sparrow: "Experiments on Heat Transfer and Pressure Drop for a Pair of Colinear, Interrupted Plates Aligned with the Flow," International Journal of Heat and Mass Transfer, 21, (1978) pp. 1069-1080.

6.) N. Cur and E. M. Sparrow: "Measurements of Developing and Fully Developed Heat Transfer Coefficients Along a Periodically Interrupted Wall," Journal of Heat Transfer, accepted for publication.

Table 1

Pressure Loss Coefficient K_p for Eight-Plate Array

	Re			
t/L	1,100	3,900	8,200	13,600
0.04	0.631	0.500	0.365	0.335
0.08	0.861	0.609	0.573	0.472
0.12	1.060	0.814	0.792	0.752

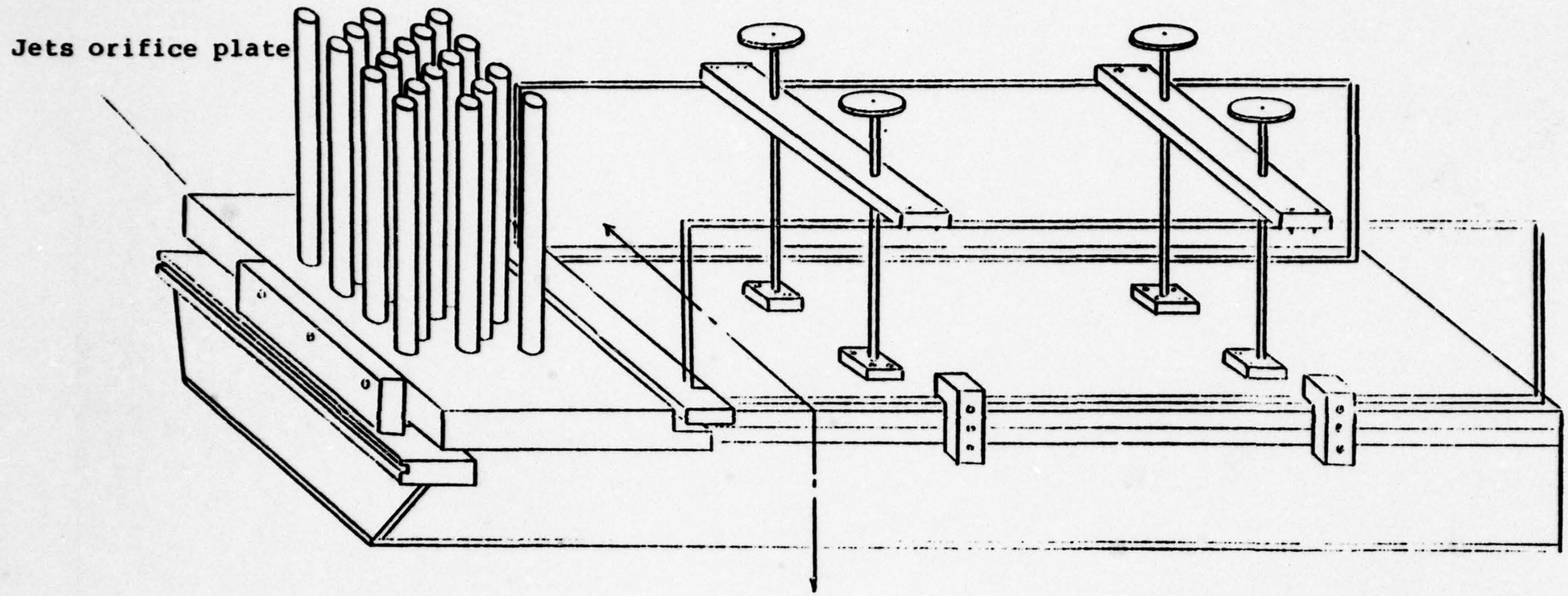

Fig. 1 Apparatus

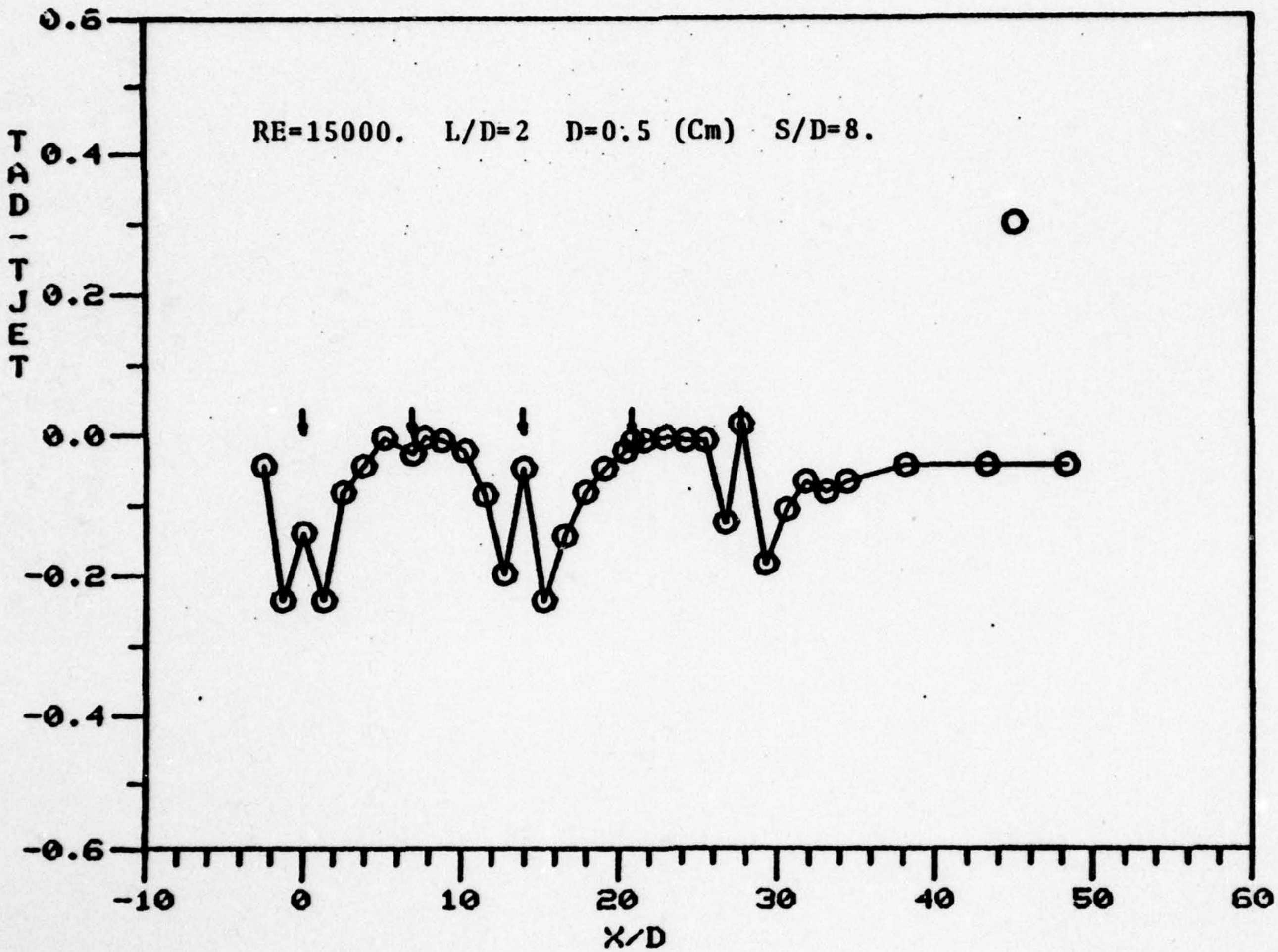
RE=15000. L/D=2 D=0.5 (Cm) S/D=8.
TAD-TJET
0.6
0.4
0.2
0.0
-0.2
-0.4
-0.6
-10
0
10
20
30
40
50
60
X/D

Fig. 2

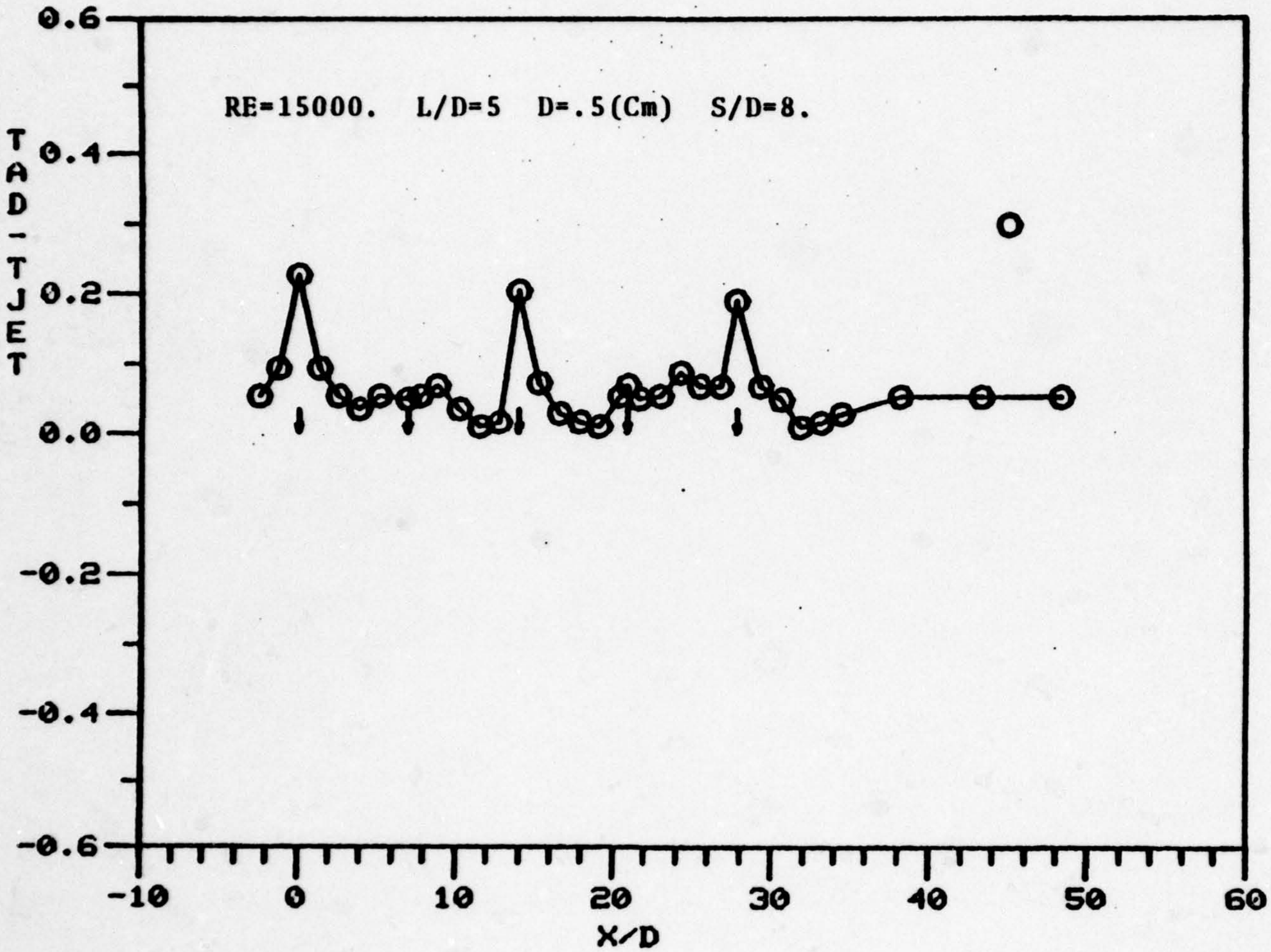
RE=15000. L/D=5 D=.5(Cm) S/D=8.
TAD-TJET
0.6
0.4
0.2
0.0
-0.2
-0.4
-0.6
-10
0
10
20
30
40
50
60
X/D

Fig. 3

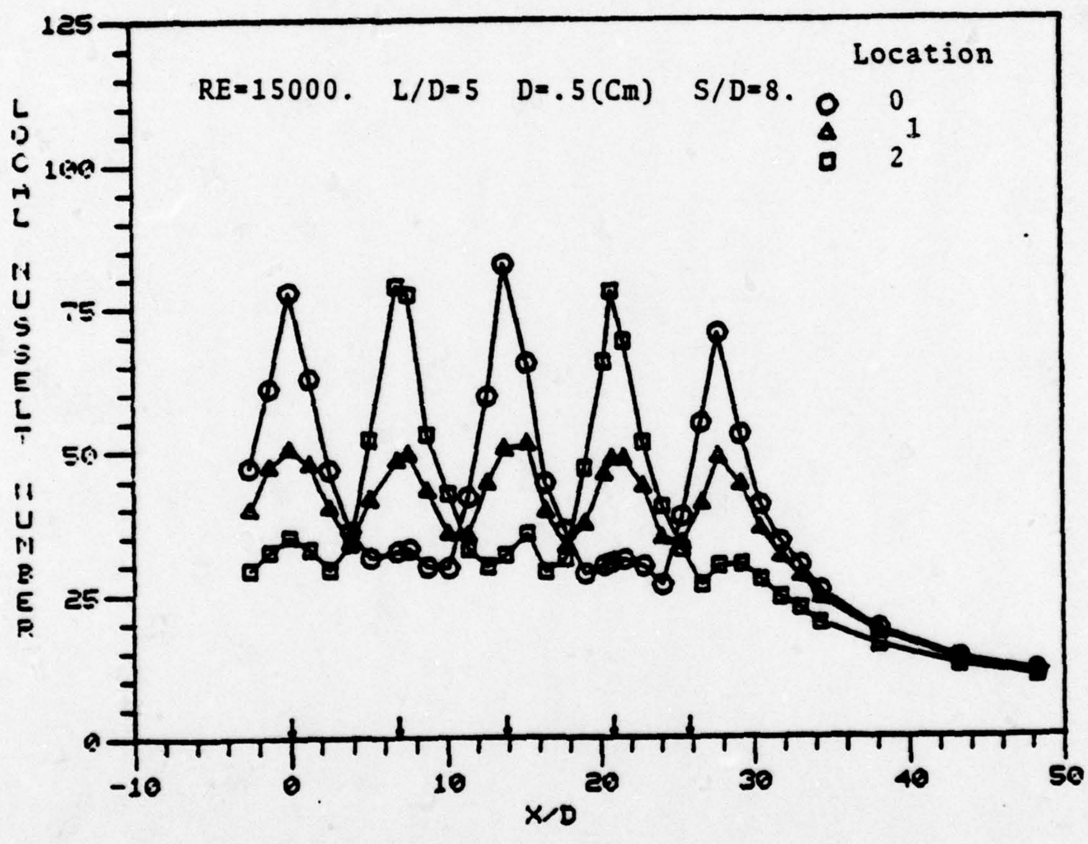

RE=15000. L/D=5 D=.5(Cm) S/D=8.
Location
0
1
2
LOCAL NUSSELT NUMBER
125
100
75
50
25
0
-10
0
10
20
30
40
50
X/D

Fig. 4

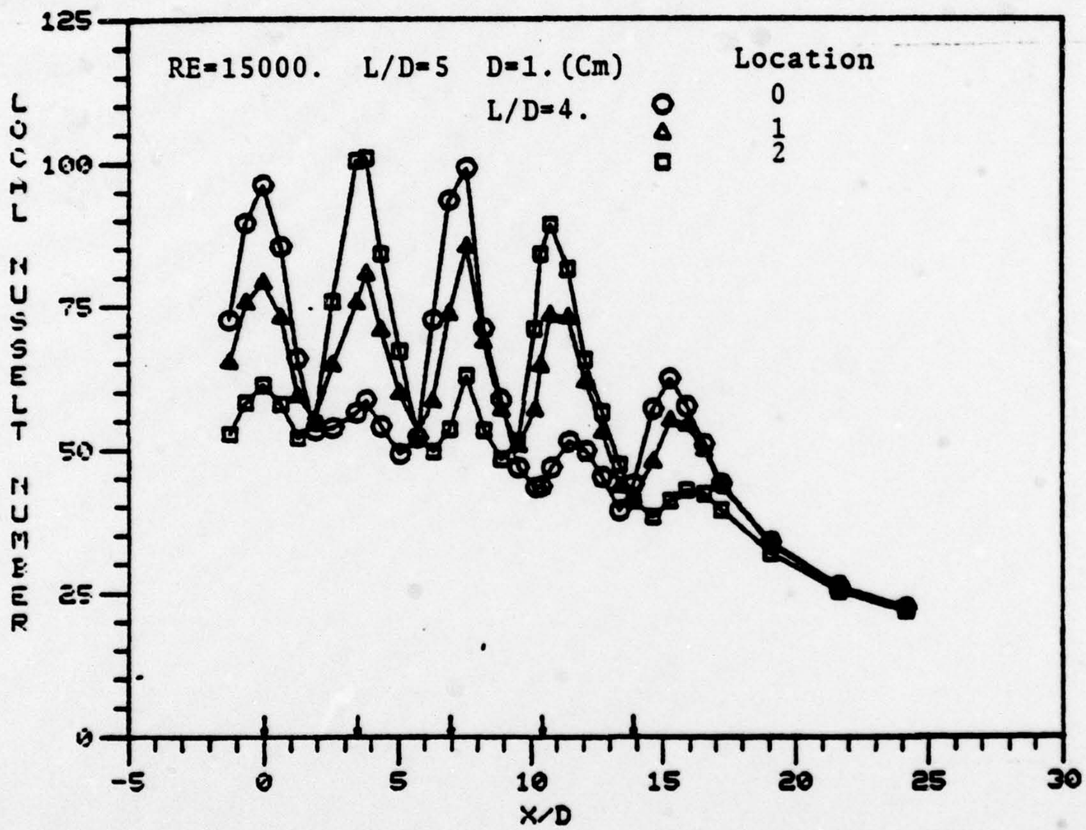
RE=15000. L/D=5 D=1.(Cm)
L/D=4.
Location
0
1
2
LOCAL NUSSELT NUMBER
125
100
75
50
25
0
-5
0
5
10
15
20
25
30
X/D

Fig. 5

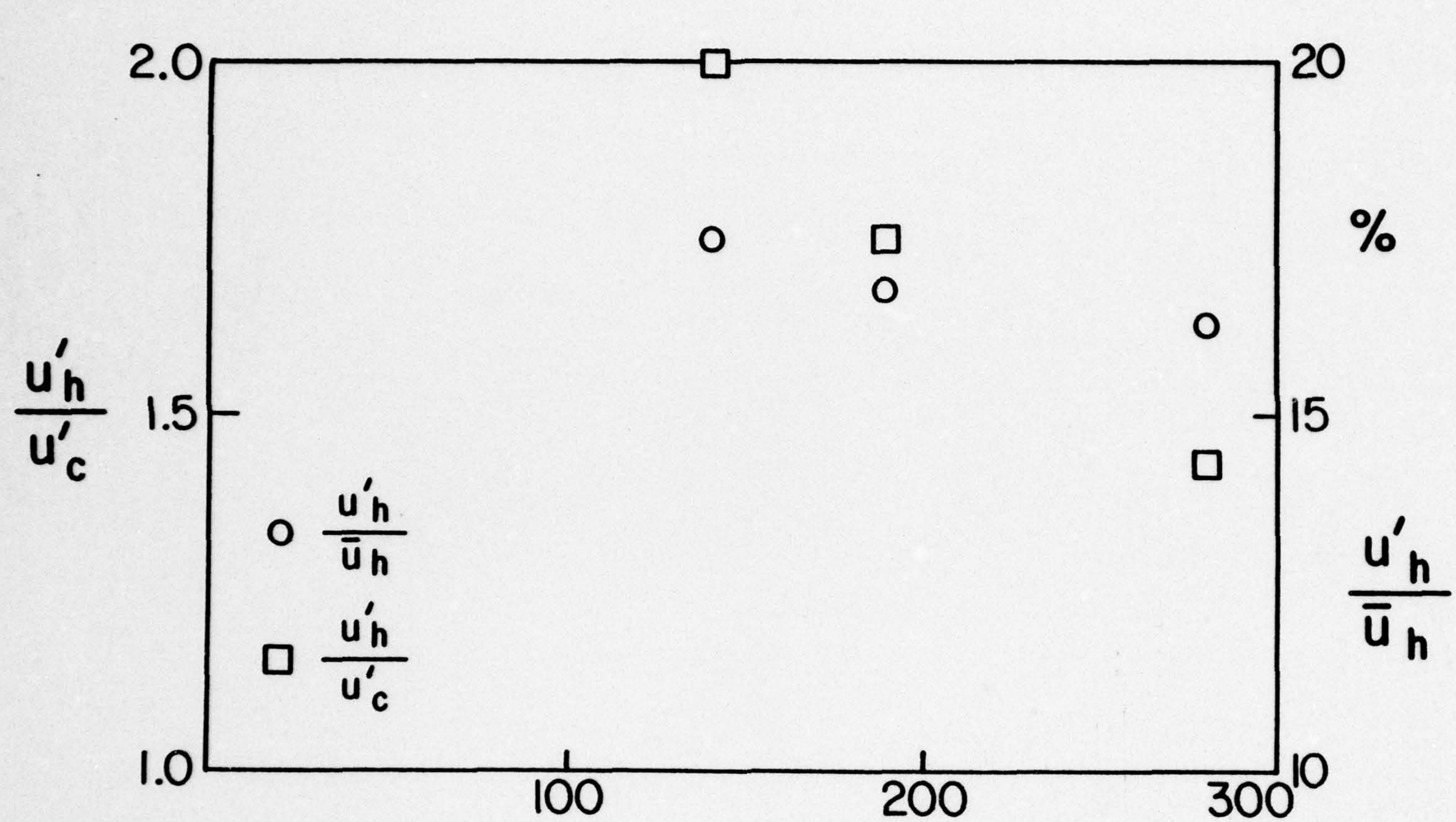
2.0
1.5
1.0
$\frac{u'_h}{u'_c}$
20
15
10
%
$\frac{u'_h}{\bar{u}_h}$
100
200
300
○ $\frac{u'_h}{\bar{u}_h}$
□ $\frac{u'_h}{u'_c}$

Fig. 6

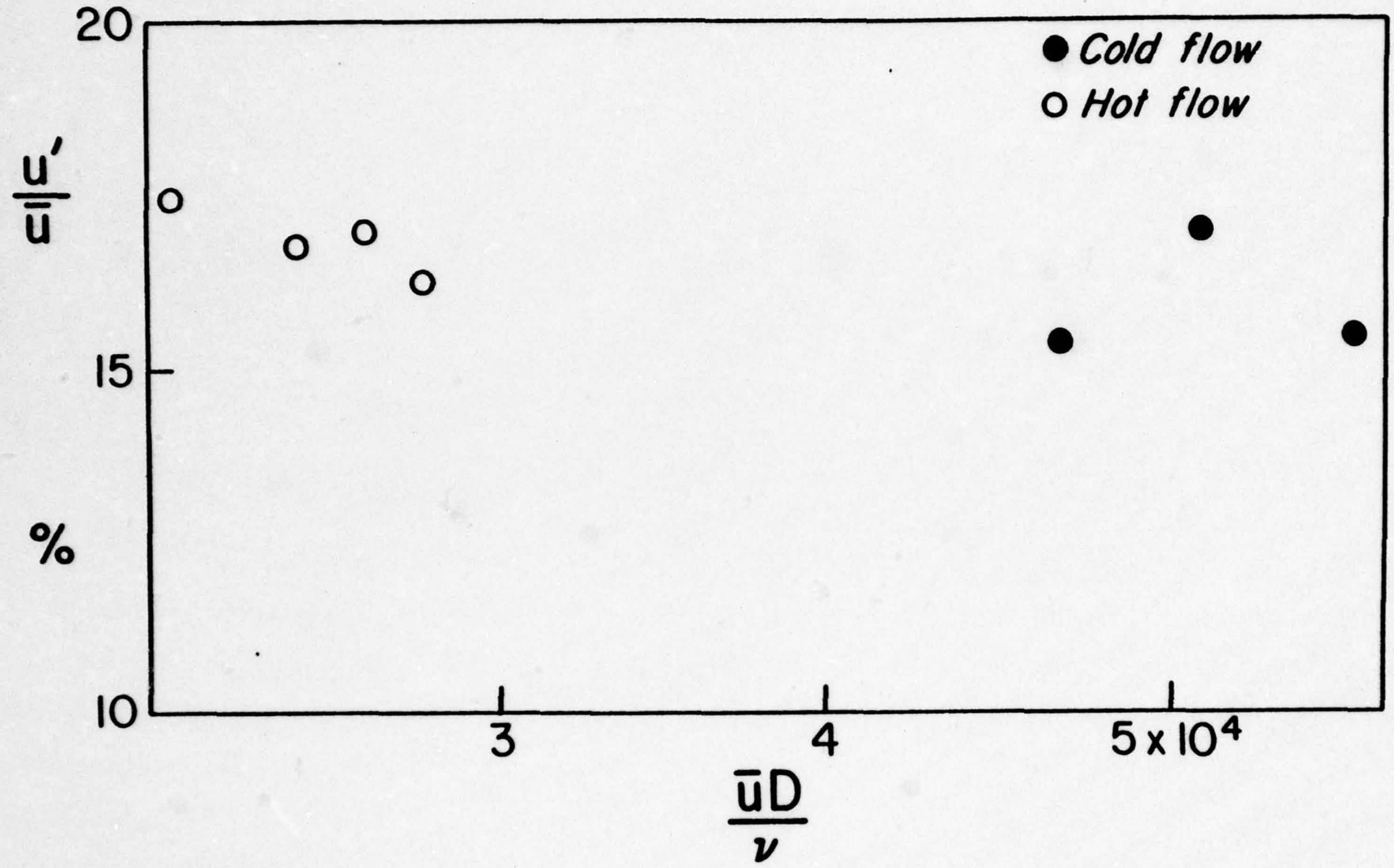

Fig. 7

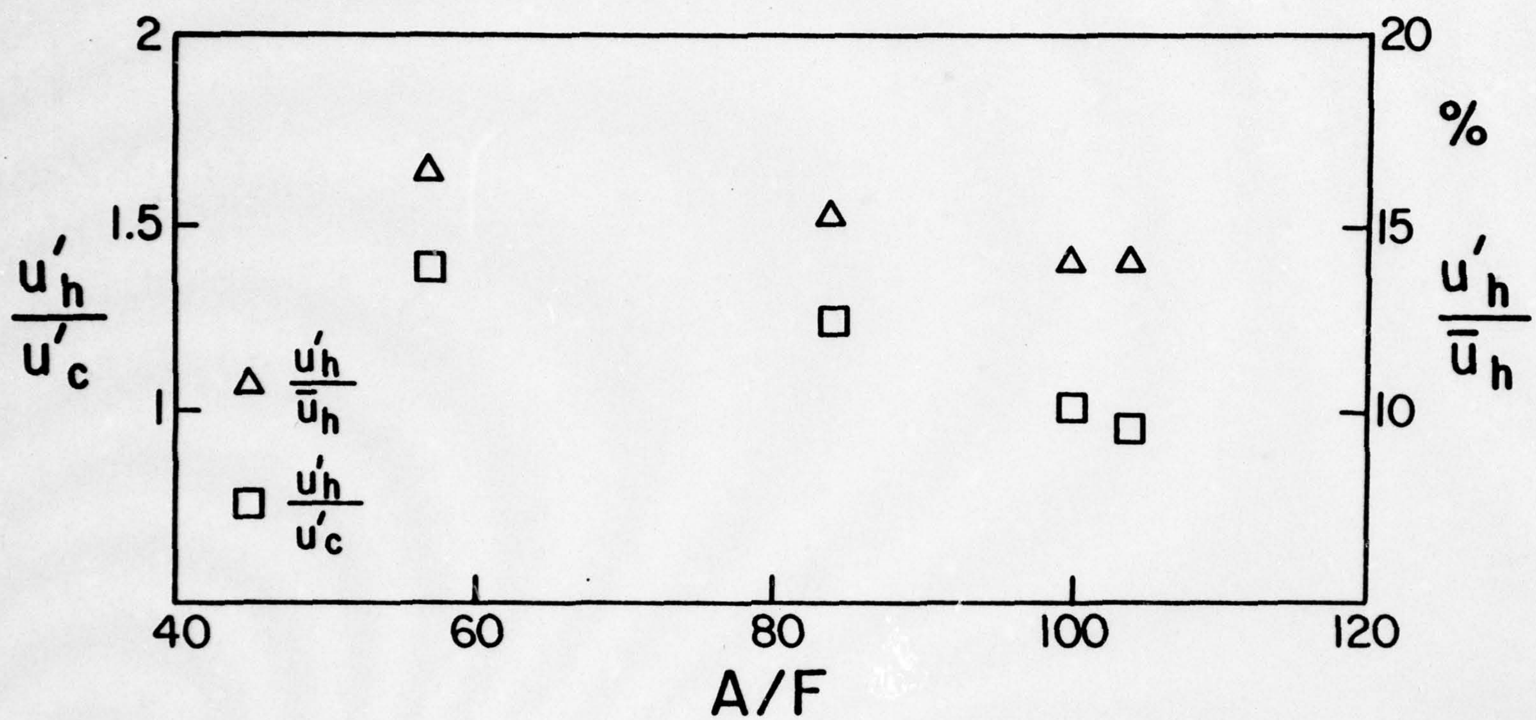

Fig. 8

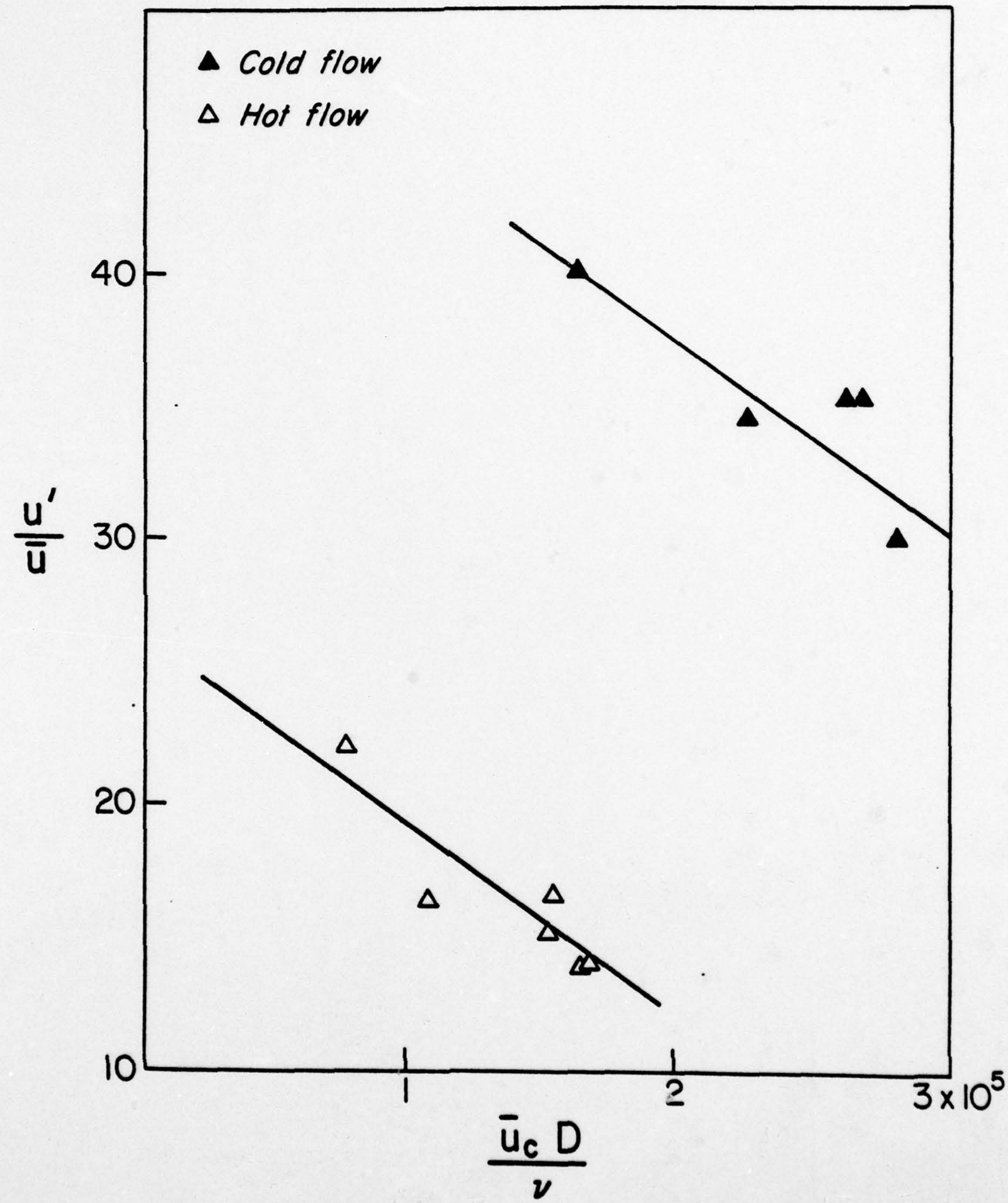

Fig. 9

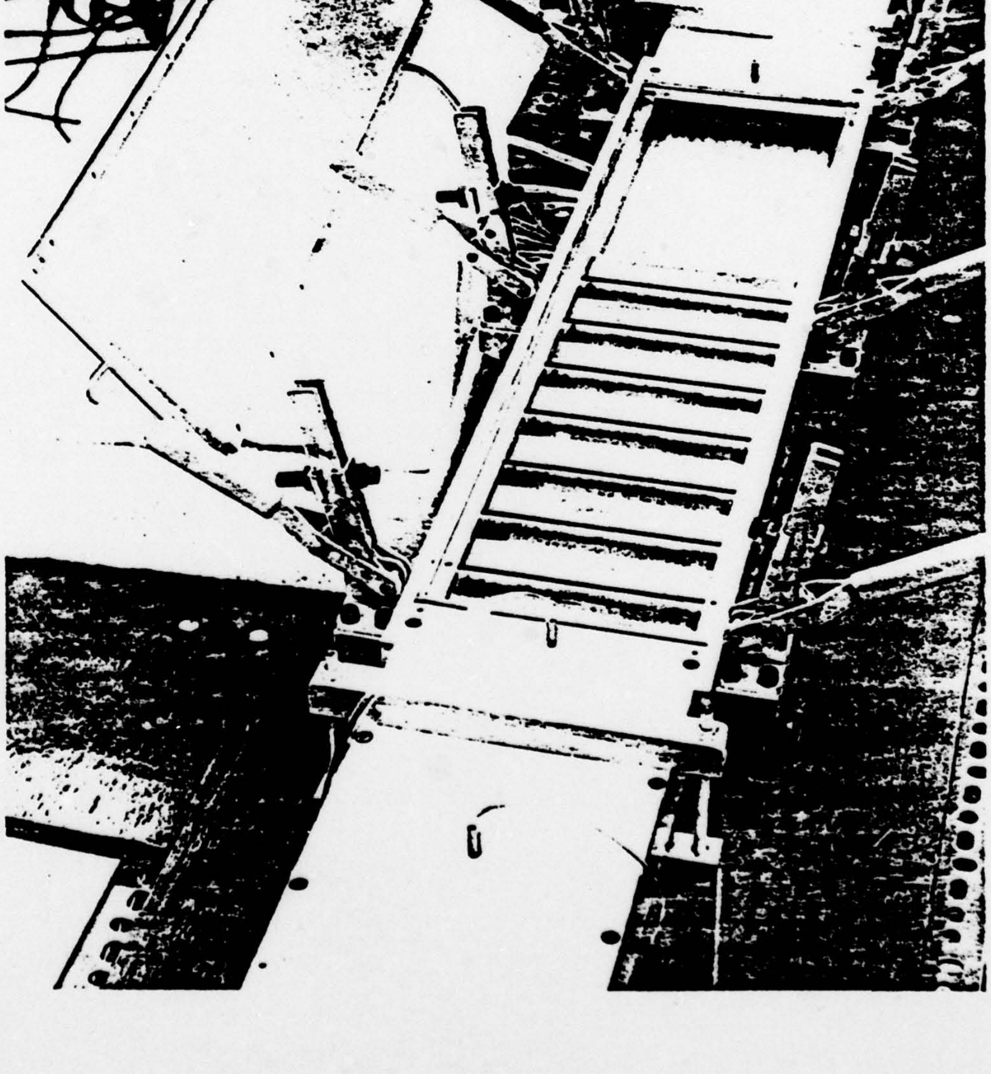

Fig. 10

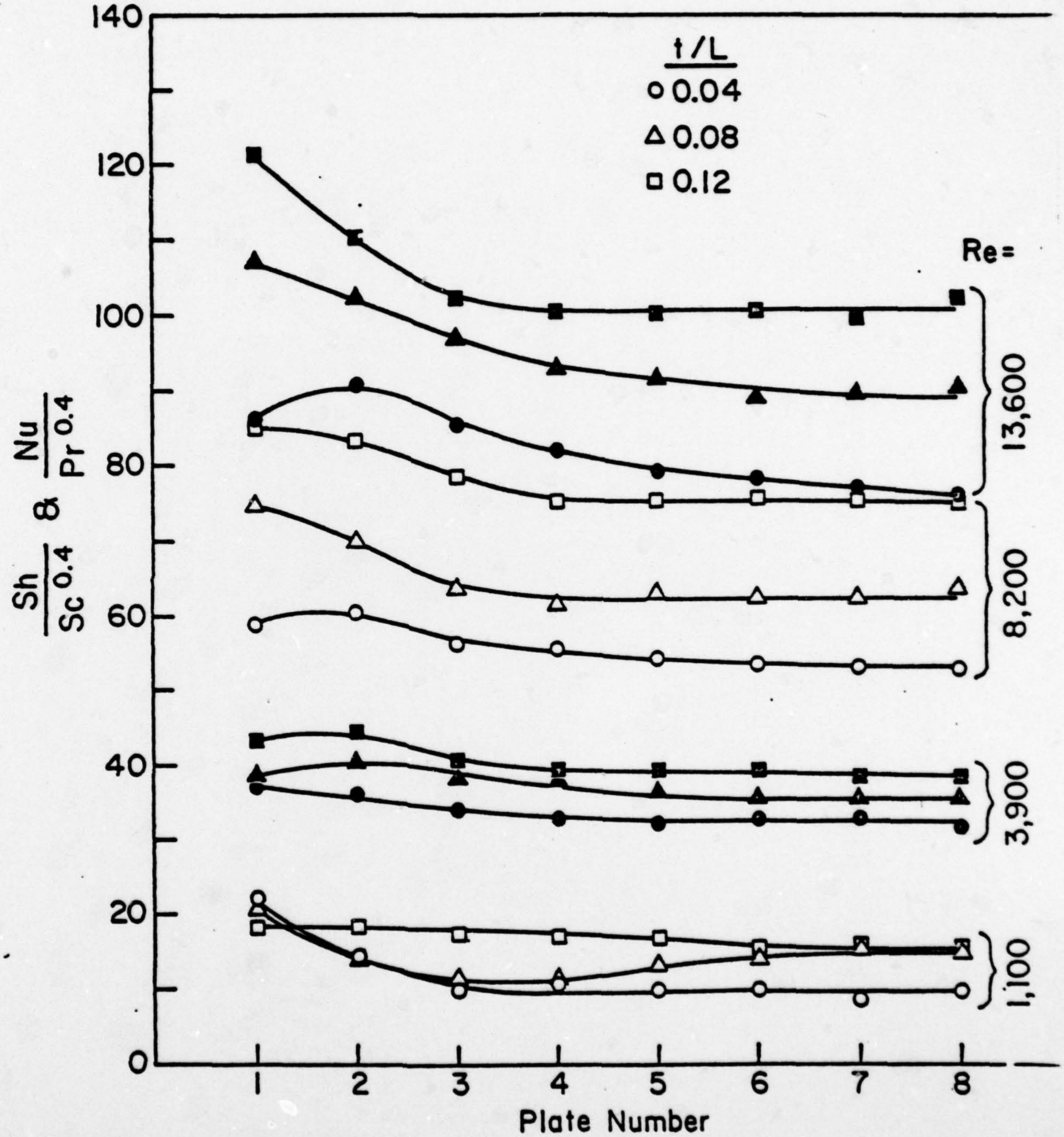

t/L
0.04
0.08
0.12
Re=
13,600
8,200
3,900
1,100
$\frac{Sh}{Sc^{0.4}}$ & $\frac{Nu}{Pr^{0.4}}$
0
20
40
60
80
100
120
140
1
2
3
4
5
6
7
8
Plate Number

Fig. 11

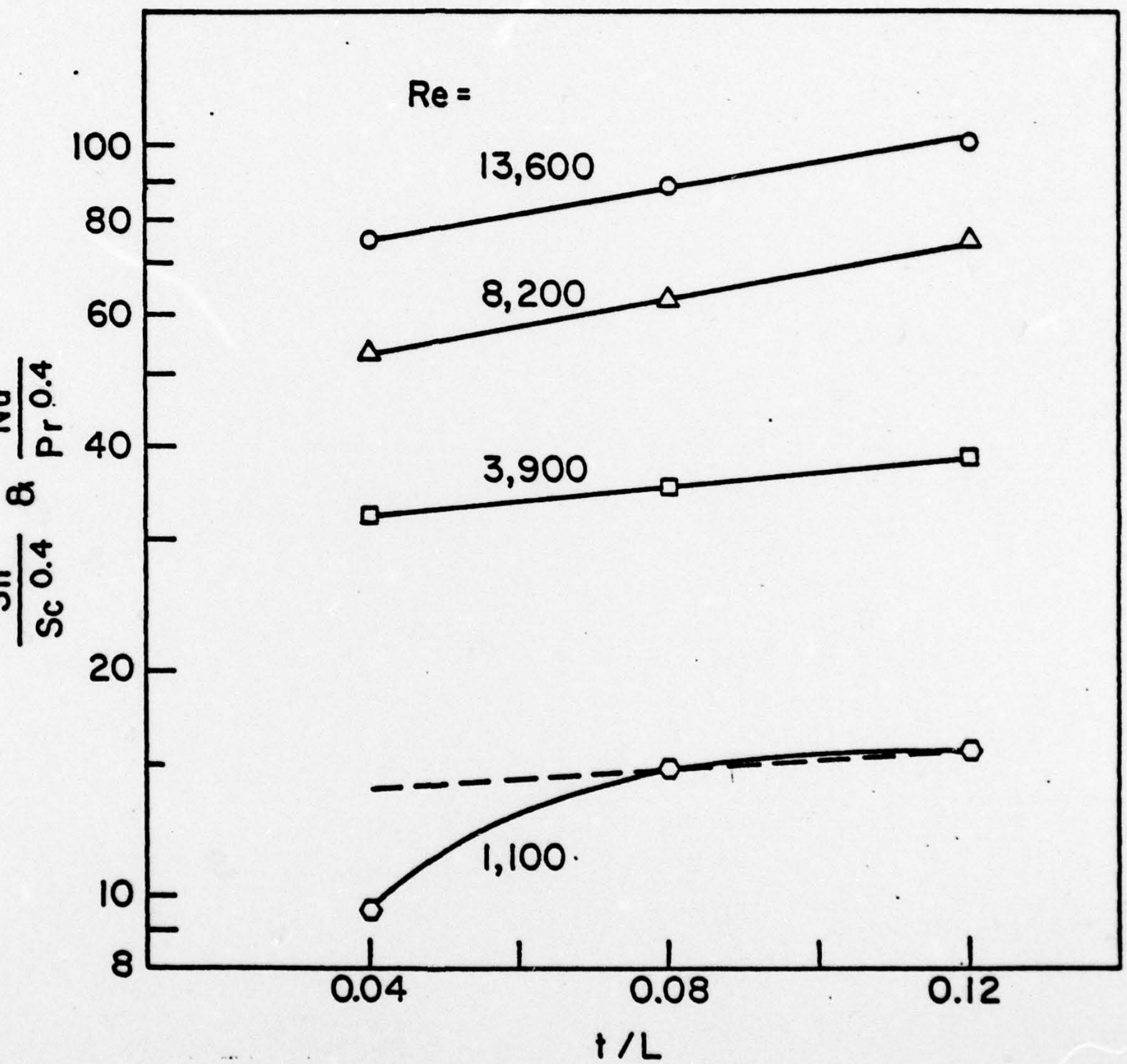
Re =
13,600
8,200
3,900
1,100
100
80
60
40
20
10
8
$\frac{Sh}{Sc^{0.4}}$ & $\frac{Nu}{Pr^{0.4}}$
0.04
0.08
0.12
t / L

Fig. 12

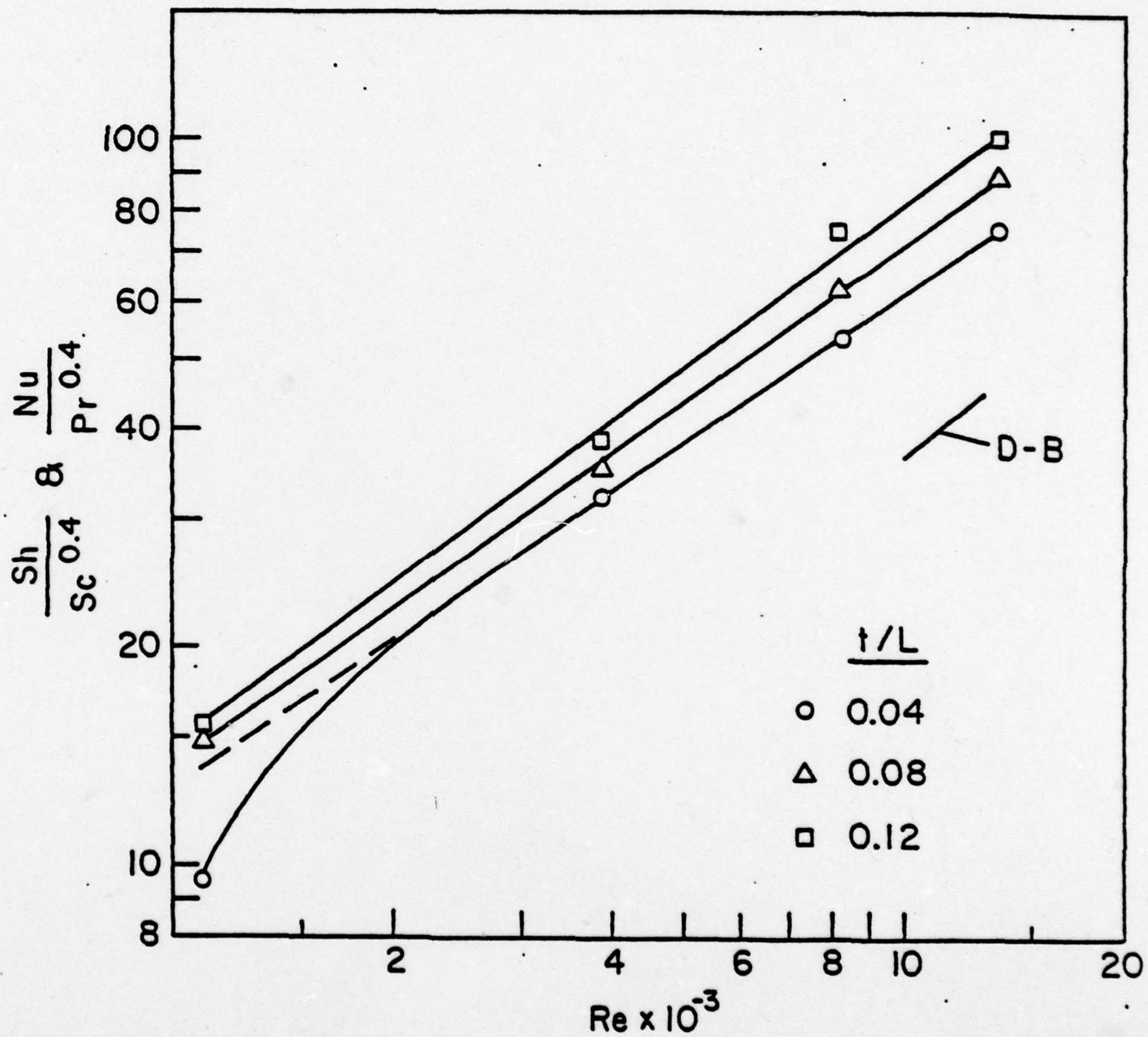

100
80
60
40
20
10
8
2
4
6
8
10
20
Re x 10^{-3}
Sh/Sc^0.4 & Nu/Pr^0.4
D-B
t/L
0.04
0.08
0.12

Fig. 13

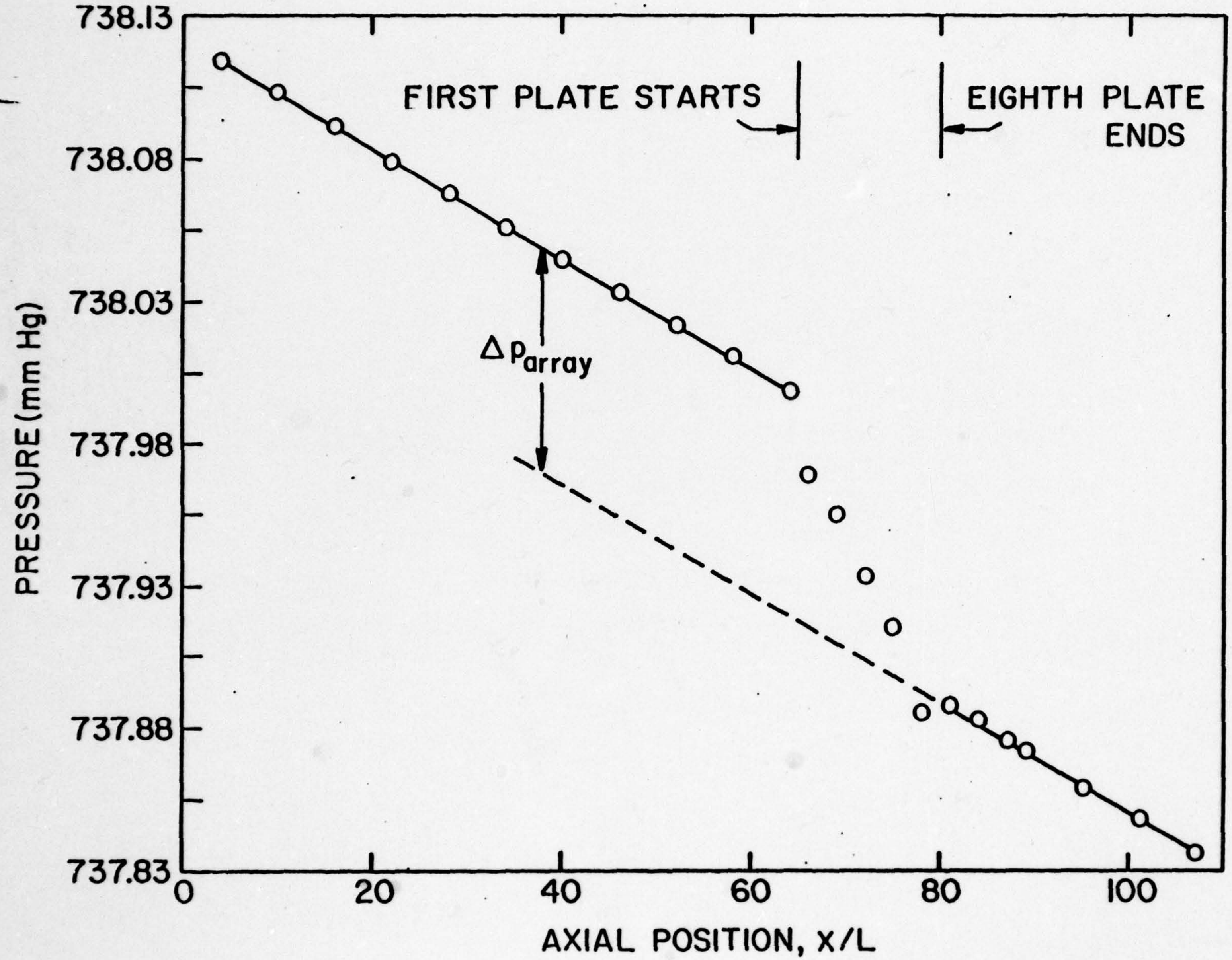

738.13
738.08
738.03
737.98
737.93
737.88
737.83
PRESSURE (mm Hg)
0
20
40
60
80
100
AXIAL POSITION, X/L
FIRST PLATE STARTS
EIGHTH PLATE ENDS
Δp_{array}

Fig. 14

473:MKE:dbw
13 Sept. 1977

DISTRIBUTION LIST

HEAT TRANSFER RESEARCH

	No. Copies
Office of Naval Research 800 N. Quincy Street Arlington, VA 22217 Attn: Power Program, M. Keith Ellingsworth Technology Group	 3 1
Defense Documentation Center Bldg. 5 Cameron Station Alexandria, VA 22314	 12
Naval Research Laboratory 4555 Overlook Ave. Washington, DC 20390 Attn: Technical Information Division	 12
US Naval Post Graduate School Monterey, CA 93940 Attn: Dept. of Mechanical Engineering Dept. of Aeronautics	 1 1
US Naval Academy Annapolis, MD 21402 Attn: Dept. of Mechanical Engineering Dept. of Aeronautics	 1 1
~~Office of Naval Research~~ ~~Branch Office~~ ~~495 Summer Street~~ ~~Boston, MA 02210~~ ~~Attn: Dr. A. D. Wood~~	 1
Office of Naval Research Branch Office 536 South Clark Street Chicago, IL 60605 Attn: Mr. M. A. Chaszeka	 1
~~Office of Naval Research~~ ~~Branch Office~~ ~~1030 East Green Street~~ ~~Pasadena, CA 91106~~ ~~Attn: Mr. B. J. Cagle~~	 1

Naval Air Systems Command
Jefferson Plaza
Washington, DC 20360
Attn: Propulsion Administrator, Code 330 1

Naval Sea Systems Command
Crystal Plaza
Washington, DC 20360
Attn: Ship Main Propulsion & Energy Br., Code 0331 1

Naval Ship Engineering Center
National Center
Washington, DC 20362
Attn: Propulsion Systems, Code 6140B 1

Naval Ship R&D Center
Annapolis, MD 21402
Attn: Power Systems Division 1
Gas Turbine Branch 1

Army Research Office
P.O. Box 12211
Research Triangle Park, NC 27709
Attn: Mr. James J. Murray 1

Air Force Office of Scientific Research
Bolling Air Force Base
Washington, DC 20332
Attn: Directorate of Aerospace Sciences 1

National Science Foundation
1800 G Street NW
Washington, DC 20550
Attn: Div. of Engineering, Heat Transfer Program 1

Energy Research & Development Administration
20 Massachusetts Ave. NW
Washington, DC 20545
Attn: Div. of Conservation Research & Technology,
Thermodynamics and Heat Transfer 1

University of Arizona
Aerospace & Mechanical Engineering Dept.
College of Engineering
Tucson, AZ 85721
Attn: Professor Don McEligot 1

Robert Mindak
Code 438
Office of Naval Research
800 N. Quincy Street 1
Arlington, VA 22217